DOI: 10.7860/JCDR/2026/78752.22214

Modelling and Simulation of Shape Memory Alloy Microactuator for Bionic Flexion Support in Older Adults: An Experimental Study

MURALIDHARAN[1], MUTHUKUMARAN[2]

ABSTRACT

Introduction: Mobility challenges among elderly people have become a concern in the healthcare and engineering sectors. One common impairment in older age is the inability to perform forward bending movements. This difficulty affects essential daily activities such as dressing and removing wearable devices, leading to reduced independence and a lower quality of life. Nitinol (NiTiNOL) is an alloy composed of approximately 45% nickel (Ni) and 45% titanium (Ti). By manipulating the thermal environment, temperature variations occur in Shape Memory Alloy (SMA) wires. SMAs are widely utilised in industry, medicine, and robotics due to their flexibility, light weight, and the ability to undergo phase transformations when subjected to thermal changes in the environment.

Aim: This research aims to model and simulate a micro SMA actuator for bionic applications.

Materials and Methods: In this experimental study, COSMOL Multiphysics software analysed the behaviour of SMA wires. Electrical excitation was used to attain the deformation temperature of the SMA wire. The modelled SMA wire, with a diameter of 0.375 mm and length of 50 mm, was simulated at the Centre for Sensors and Control Systems Laboratory, Hindustan Institute of Technology and Science, Chennai.

Results: The SMA microactuator exhibits notable thermal behaviour linked to phase transformations and mechanical properties. The modelled SMA spring features three turns, a diameter of 0.375 mm, and a length of 50 mm. It operates between 40°C and 65°C, with the austenite temperature at 65°C. These parameters yield an actuation force of 9.31 N and a displacement of 20.3 mm.

Conclusion: The simulation results have been used to develop a soft robot for clinical purposes and bionic applications. To address such biomechanical deficits, an SMA-based actuator offers compact, quiet, and flexible motion in wearable or embedded assistive systems.

Keywords: Biomechanical movements, COMSOL multiphysics Embedded assistive system, Joule heating, Soft robot

INTRODUCTION

The SMA is commonly known as a smart material and a transducer. Nitinol (NiTiNOL) is one of the smart materials used in commercial and biomedical applications [1]. This SMA contracts in length when heated. To provide a thermal environment for SMA, a continuous heat source must be supplied [2,3]. A bidirectional soft glove integrated with SMA actuators has been developed to support finger flexion and extension for stroke or arthritis patients, providing effective hand rehabilitation support [4,5]. SMA-based artificial muscles and joints have been implemented in prosthetic limbs and robotic hands to restore dexterity and motion in amputees and individuals with musculoskeletal disorders [6]. The SMA actuators respond to temperature changes; these changes induce a transformation in its shape [7]. The SMA wire is supplied with a controlled electrical current to overcome its nonlinear behaviour. Actuation depends on PWM signal variation [8]. SMA is a popular material for robotics, automotive applications, and biomedical industries due to its softness, small form factor, and high strength-to-weight ratio. Electrically controlling SMA is a challenge in practical applications due to its nonlinear behaviour [9]. SMA has two phases in its thermal environment: the Martensitic phase at low temperature and the Austenitic phase at high temperature [10,11]. The SMA wire recovers its original shape once the current is removed, provided it is preloaded with a mechanical bias [12]. Variable stiffness actuators [13], motion-supporting bionic structures using materials such as Polydimethylsiloxane (PDMS)/Aluminium Oxide (Al_2O_3) composites [13,14], dielectrics for capacitive pressure sensors [15], prosthetics, exoskeletons, and actuation of joint mechanisms [16], are used for bionic applications with electronic control. In such applications, actuator stiffness is achieved by electrically controlled SMA wires guided by the mechanical structure. The generated force and displacement characteristics of the designed SMA microactuator using COMSOL Multiphysics are presented. The seamless integration of soft robotic systems facilitates the creation of SMA micro-actuated biomedical devices such as soft robotic gloves, prosthetic joints, and therapeutic exosuits, delivering safe adaptive support for individuals with motor function impairments [5,17]. The proposed modelling and simulation of SMA microactuators motivate the development of actuators that provide flexible embedded assistive systems. This study aims to provide electrically controlled actuation for devices usable by older people who require biomechanical assistance in their day-to-day activities.

MATERIALS AND METHODS

In the present experimental study, the modelled SMA wire, with a 0.375 mm diameter and 50 mm length, was simulated at the Centre for Sensors and Control Systems Laboratory, Hindustan Institute of Technology and Science, Chennai.

COMSOL Multiphysics is a powerful software used to perform simulations in the temperature range 40°C to 65°C. The actuating force of 9.31 N and a displacement of 20.3 mm were obtained from the simulation results.

Behavioural Study of the SMA Spring under Thermal Environment

The SMA spring produces displacement in response to the applied force. An SMA spring-actuated system exhibits nonlinear elastic behaviour, which can be described by

$$F=k(x)x^n \quad (1)$$

The SMA spring is placed in the centre of the designed cylindrical guide structure, and the total thermal response due to the electrical excitation is shown in [Table/Fig-1a].

Simulation responses of the electrically excited SMA spring with ground potential are shown in [Table/Fig-1b], and the impact of applying a positive terminal current on the SMA spring response is shown in [Table/Fig-1c]. SMA spring expansion is observed as half of the length for the selected composition of SMA material [Table/Fig-2]. A nonlinear elastic material exhibits a specific force-displacement relationship based on the applied force F, a stiffness k, and an exponent n describing material properties for the proposed SMA microactuator [Table/Fig-3]. The displacement x varies during actuation due to SMA properties. The spring constant influences the two phase transitions as temperature changes. In the proposed SMA actuating system, an SMA wire is used in the form of a spring. The effective spring constant of the SMA spring attached to the mechanical guide structure is temperature-dependent and governed by the phase state of the material.

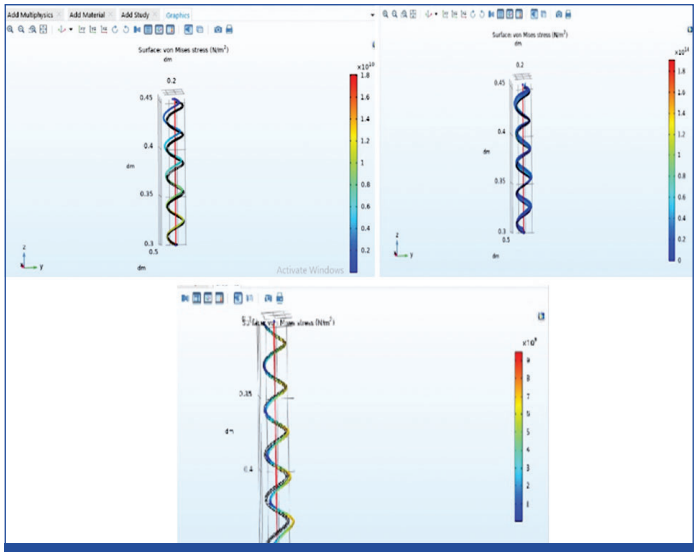

[Table/Fig-1]: (a) Simulation of SMA spring with electrical excitation. (b) Response of SMA spring at ground potential. (c) Response of SMA spring at terminal voltage.

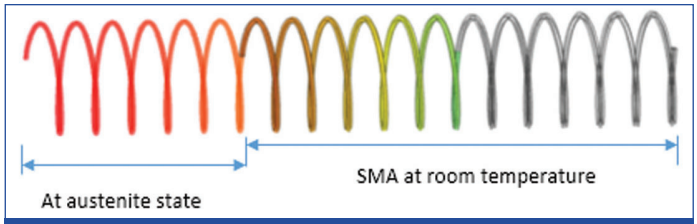

[Table/Fig-2]: Deformation of SMA wire.

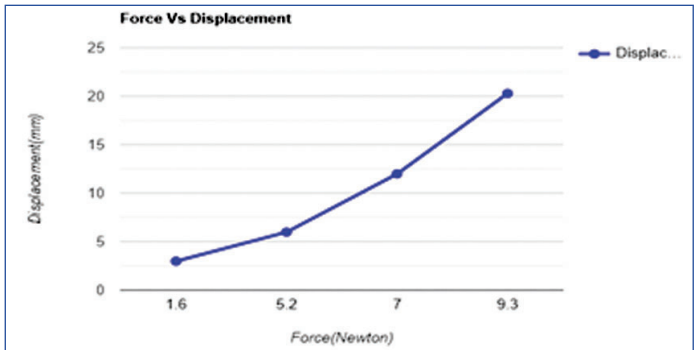

[Table/Fig-3]: Force-displacement relationship for designed SMA microactuator.

A non-linear elastic material exhibits a specific force-displacement relationship based on an applied force of 'F', a stiffness 'k', and 'n' material properties for the proposed SMA microactuator [Table/Fig-3]. The displacement 'x' varies during actuation due to SMA properties. The spring constant influences two phase transitions according to temperature changes. In the proposed SMA actuating system, an SMA wire is used in the form of a spring. The effective spring constant of the SMA spring attached to the mechanical guide structure is,

$$k=(E \bullet A) / L \quad (2)$$

Where, the stiffness of the SMA spring attached structures mechanical guide depends on elastic modulus '*E*', cross-sectional *area A*', length of SMA wire '*L*'. SMA spring's strain, prestrain is analysed at load and no load conditions.

Strain and Prestrain in SMA Spring Microactuator

Quotient of change in length 'ΔL' and original Length 'L_0' provides strain 'ε' of a SMA microactuator.

$$\varepsilon=\frac{\Delta L}{L_0} \quad (3)$$

Stress 'σ' imposed due to elastic strain '$\varepsilon_{elastic}$'. Fraction of 'ε' strain develops deformation in SMA spring. Transformation strain 'ε_{trans}' is added due to the mechanical guide structure.

Prestrain is typically imposed by elongating the SMA spring beyond the elastic region up to desired level of transformation strain.

The transformation strain 'ε_{trans}' for proposed SMA microactuator is the product of maximum elongation strain '$\varepsilon_{elongation}$' at austenite state and martensite state.

$$\varepsilon_{trans}=\varepsilon_{max}.\varepsilon \quad (4)$$

The elongation at prestrain is the calculated from the change in length and original length of SMA spring.

$$\varepsilon_{pre}=\frac{\Delta L_{pre}}{L_0} \quad (5)$$

The total prestrain of SMA spring standard of designed SMA microactuator obtained from equation (4), equation (5) and the standard plastic strain '$\varepsilon_{plastic}$'.

$$\varepsilon_{pre}=\varepsilon_{elastic}+\varepsilon_{trans}+\varepsilon_{plastic} \quad (6)$$

The difference in strain between loading ($\varepsilon_{loading}$) and unloading ($\varepsilon_{unloading}$) is proportional to the hysteresis width, prestrain kept below 8%. Both strain and prestrain effects are temperature dependent due to phase transformation (martensite - austenite).

The stiffness of the designed SMA spring attached mechanical guide structure is,

$$k(x)=\frac{F}{x^n} \quad (7)$$

The Work done at SMA spring attached mechanical guide structure in terms of force is,

$$W=F.dx \quad (8)$$

The Force generated by the SMA spring attached mechanical guide is obtained from the equation (7), and replacing it in equation (8) the work done is,

$$W=k(x)\, x_n.dx \quad (9)$$

To substitute k(x) as k_0,

$$W=k_0\, x_n\, dx \quad (10)$$

$$w=k_0\,\frac{x^n+1}{n+1}\ C \quad (11)$$

The stiffness derivative of SMA spring attached mechanical guide structure, if k(x) itself depends on $k(x)=k_0x^m$, then

$$F=k_0x^m\, x^n \quad (12)$$

$$k(x)=\frac{F}{x^n}=\ k_0x^m \quad (13)$$

The force imposed due to stiffness of SMA spring becomes,

$$F=k_0\, x^{m+n} \quad (14)$$

Work done for the variable stiffness due to transformation of SMA microactuator can be written as

$$W=k_0 x^{m+n} dx \quad (15)$$

$$W=\frac{x^{m+n+1}}{m+n+1} \quad (16)$$

Hence the developed system is dynamic, Newton's second law relates the force to mass 'm' and acceleration 'a'

$$F=m\frac{(d^2x)}{dt^2} \quad (17)$$

From equation (17) and equation (7),

$$m\frac{(d^2x)}{dt^2}=k(x)x^n \quad (18)$$

$$m\frac{(d^2x)}{dt^2}=k_0x^n \quad (19)$$

Total span of individual spherical structure within the designed mechanical guide is [Table/Fig-4].

$$S=N.(2rd) \quad (20)$$

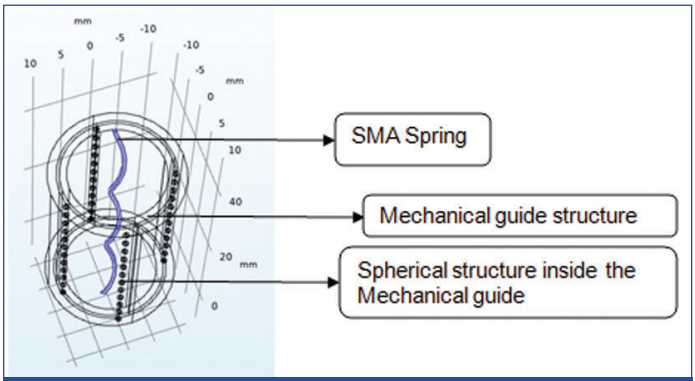

[Table/Fig-4]: COMSOL design of SMA microactuator.

Experimental Set-up for SMA Spring Microactuator

[Table/Fig-5a] SMA spring expansion; [Table/Fig-5b]: SMA spring suppression.

Impact of Kinematics in spherical structure due to dynamic movement of developed mechanical guide at the time of actuation is obtained from the velocity 'v',

$$v=r\omega \quad (21)$$

Radius of the spherical structure is 'r'and angular velocity of the spherical structure is 'ω'. The forces acting on the spherical structure is precise on the SMA spring attached mechanical guide structure. Those are Constant force (F_c), Frictional force (F_f), and Inertial force (F_i)

Total force on each spherical structure inside the designed mechanical guide is,

$$F=F_c+F_f+F_i \quad (22)$$

The spherical structure of designed to create actuation in mechanical guide. This structure creates the moment of inertia in SMA spring microactuator [Table/Fig-5]. The created moment of inertia will act at the centre of the spherical structure. That is,

$$I=\frac{2}{5}mr^2 \quad (23)$$

Mass of a single spherical structure inside the designed mechanical guide is,

$$m=\rho v \quad (24)$$

$$m=\rho\frac{4}{3}\pi r^3 \quad (25)$$

STATISTICAL ANALYSIS

Descriptive statistics were used to analyse the data.

The SMA spring microactuator responds to the applied voltage (V) using controlled electric pulses, as shown in [Table/Fig-5]. The switching time can be varied by a microcontroller that generates 255 pulses per second. Additionally, temperature variations are observed in relation to the changing electric current [Table/Fig-6,7].

The proposed SMA microactuator exhibited interesting thermal behaviour, particularly related to phase transformations and the mechanical properties of the selected material composition.

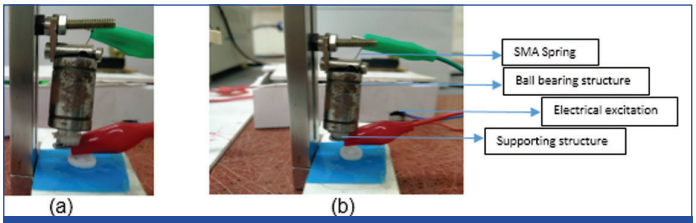

[Table/Fig-5] (a) SMA spring expansion; (b) SMA spring suppression.

Voltage (Volts)	Current (Ampere)	Power dissipation (Watts) P=VI	Calculated Temperature (°C)	Observed temperature (°C)
12.50	0.30	3.75	42.51	42.3
12.50	0.60	7.50	52.24	50.4
12.50	0.90	11.25	61.97	58.6
12.50	1.20	15.00	71.70	69.3

[Table/Fig-6]: Temperature observed for different current rating.

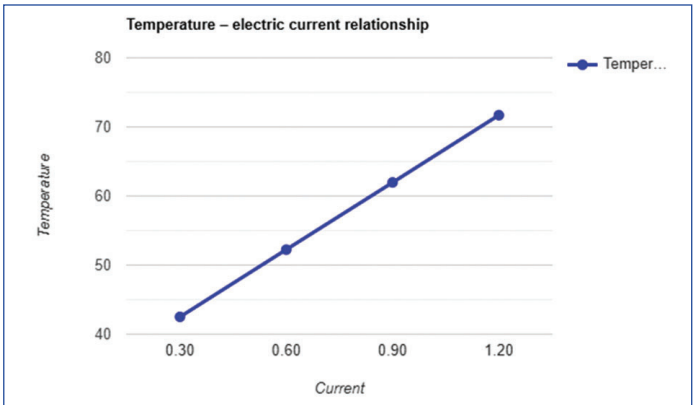

[Table/Fig-7]: Temperature - electric current relationship.

SMA structures are often polycrystalline, consisting of small crystalline grains with different orientations. This microstructure significantly influences the SMA spring's overall behaviour, including its thermal response. Conducting simulations on such software allows modelling of complex systems and understanding their behaviour under different conditions.

The modelled SMA spring has three turns, a 0.375 mm diameter, and a 50 mm length. The operating temperature range of 40°C to 65°C is fixed as per the preheat treatment of the SMA wire. The austenite temperature is 65°C. These simulation parameters produce an actuation force of 9.31 N and a displacement of 20.3 mm in the designed SMA microactuator. The accompanying colour scale illustrates that lower values are indicated by orange, while higher values are represented in violet. This gradient visualises the distribution of the temperature field in the simulation results. Different colours correspond to distinct response ranges, where orange indicates higher force values and violet indicates lower force values [Table/Fig-8].

DISCUSSION

The simulation and modelling of the SMA microactuator reveal critical insights into its thermal and mechanical behaviour, particularly in the context of bionic support systems for elderly individuals. The operating temperature range of 40°C to 65°C is carefully selected based on the pre-processing of the NiTiNOL wire, ensuring optimal phase transformation between martensite and austenite states. This transformation is essential for achieving reliable actuation and restoring shape-memory properties under controlled electrical excitation [18].

A key observation is the influence of the supporting structure on thermal resistivity. The manuscript highlights that porcelain, due to its superior thermal compatibility, may outperform conventional high-

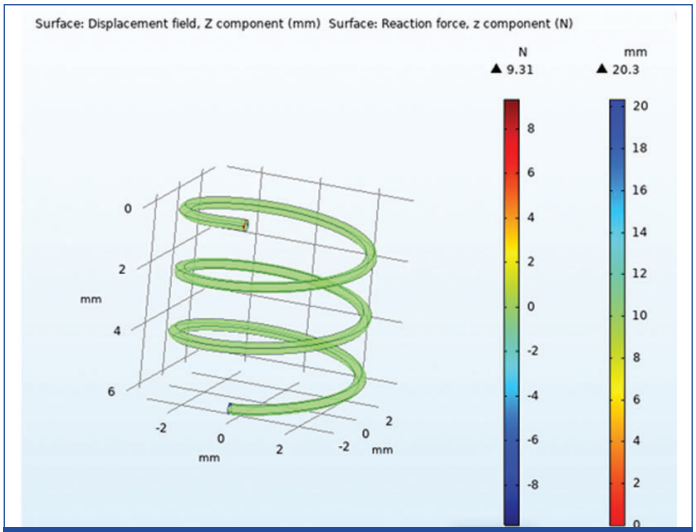

[Table/Fig-8]: Simulation result of the SMA spring.

fabric glass materials currently used in ball-bearing structures. This substitution could enhance the actuator's durability and thermal stability, especially under repeated cycles of heating and cooling [19].

The Pulse Width Modulation (PWM) technique used for electrical control plays a pivotal role in managing the actuator's response time and force generation. The study suggests that optimizing PWM parameters and the skeleton design of the Micro-Electro-Mechanical Systems (MEMS) actuator can significantly improve system performance, especially in wearable applications where precision and safety are paramount.

Moreover, the simulation results showing a force output of 9.31 N and a displacement of 20.3 mm demonstrate the actuator's potential for integration into assistive devices such as soft robotic gloves, prosthetic joints, and therapeutic exosuits. These devices can offer adaptive support for individuals with motor impairments, enhancing mobility and independence in daily activities [20,21].

Additionally, the microstructural characteristics of SMA note that its polycrystalline nature affects thermal response and mechanical properties. This underscores the importance of material selection and pretreatment in actuator design [6].

The proposed SMA microactuator system is not only thermally responsive and mechanically efficient but also adaptable for real-world bionic applications. Future work may explore advanced materials, refined control strategies, and integration with sensor feedback systems to further enhance its utility in clinical and rehabilitative settings.

Limitation(s)

Constant current distribution maintenance is a major challenge in proposed system due to the usage of conventional PWM technique.

CONCLUSION(S)

This study presents dynamic and thermal analyses of the SMA spring microactuator with specified dimensions, highlighting its potential for applications in soft robotics, medical devices, bio-inspired systems, and bionic applications. The generated force and displacement support GRASP-Graded Repetitive Arm Supplementary Program (GRASP)-assist movements for elderly users and rehabilitation devices with controlled motion and grip enhancement.

REFERENCES

[1] Pei YC, Wang BH, Wu JT, Wang C, Guan JH, Lu H. A machine learning empowered shape memory alloy gripper with displacement-force-stiffness self-sensing. IEEE Transactions on Industrial Electronics. 2022;70(10):10385-395.
[2] Mandolino MA, Scholtes D, Ferrante F, Rizzello G. A physics-based hybrid dynamical model of hysteresis in polycrystalline shape memory alloy wire transducers. IEEE/ASME Transactions on Mechatronics. 2023;28(5):2529-40.
[3] Shougat MREU, Kennedy S, Perkins E. A self-sensing shape memory alloy actuator physical reservoir computer. IEEE Sensor Letters. 2023;7(5):6002304.
[4] Bai F, Zhang X, Xu D. Accurate position tracking control of SMAAs based on low-complexity self-sensing model and compound control strategy. IEEE Sensors Journal. 2023;23(3):2280-90. Doi: 10.1109/JSEN.2022.3227293.
[5] Lai J, Song A, Shi K, Ji Q, Lu Y, Li H. Design and evaluation of a bidirectional soft glove for hand rehabilitation-assistance tasks. IEEE Transactions on Medical Robotics and Bionics. 2023;5(3):730-40. Doi: 10.1109/TMRB.2023.3292414.
[6] Baek H, Khan AM, Bijalwan V, Jeon S, Kim Y. Dexterous robotic hand based on rotational shape memory alloy actuator-joints. IEEE Transactions on Medical Robotics and Bionics. 2023;5(4):1082-92.
[7] Hyeon K, Chung C, Ma J, Kyung KU. Lightweight and flexible prosthetic wrist with shape memory alloy (SMA)-based artificial muscle and elliptic rolling joint. IEEE Robotics and Automation Letters. 2023;8(11):7849-56.
[8] Yu Y, Zhang C, Wang C, Zhou M. Neural network adaptive control of magnetic shape memory alloy actuator with time delay based on composite NARMAX Model. IEEE Transactions on Circuits and Systems-I: Regular Papers. 2023;70(8):3336-46.
[9] Patterson ZJ, Sabelhaus P, Majidi C. Robust control of a multi-axis shape memory alloy-driven soft manipulator. IEEE Robotics and Automation Letters. 2022;7(2):2210-17.
[10] Shah SIH, Shah SS, Bernharðsson E, Koziel S. Shape Memory alloy-based fluidically reconfigurable metasurfaced beam steering antenna. IEEE Access. 2023;11:102271-78.
[11] Hu Q, Dong E, Sun D. Soft modular climbing robots. IEEE Transactions on Robotics. 2023;39(1):399-416. Doi: 10.1109/TRO.2022.3189228.
[12] Hu Q, Li J, Dong E, Sun D. Soft scalable crawling robots enabled by programmable origami and electrostatic adhesion. IEEE Robotics and Automation Letters. 2023;8(4):2365-72.
[13] Milazzo G, Lemerle S, Grioli G, Bicchi A, Catalano MG. Design, characterization, and validation of a variable stiffness prosthetic elbow. IEEE Transactions on Robotics. 2025;41:82-95.
[14] Wang R, Zhang C, Zhang Y, Yang L, Qin H, Zhang Q, et al., Soft manta ray robot based on bilateral bionic muscle actuator. IEEE Robotics and Automation Letters. 2024;9(9):7723-30.
[15] Guo X, Zhao J, Hu B, Li J, Tao J, Chen Y. Flexible pressure sensor with high sensitivity and fast response based on bionic honeycomb-structured polydimethylsiloxane/aluminium oxide composites dielectric via 3-d printing. IEEE Transactions on Electron Devices. 2024;71(7):4283-91.
[16] Chen W, Ma Y, Ren L, Liang W, Wang X, Zhang Y et al. A lightweight powered knee prosthesis replicating early-stance knee flexion during level walking. IEEE Robotics and Automation Letters. 2024;9(11):9693-00.
[17] Jiang Z, Lu Y, Xie X, Shi L, Chen C, Zhang J. Design of an actuator controller based on frequency feed forward parameter compensation. in IEEE Access, 2024.
[18] Singh K, Khosla A, Gupta S, Furukawa H. Stiffness control of laminar jammers with fused layers: A discrete approach. IEEE Robotics and Automation Letters, April 2024.
[19] Li L, Xu J, Li Q, Jiang Y, Dong X, Ding J. Small multi-attitude soft amphibious robot. In IEEE Robotics and Automation Letters, Feb. 2024.
[20] Yang Y, Feng Z, Ma S, Tang L, Jin C, Li Y. The continuous jump control of a locust-inspired robot with omnidirectional trajectory adjustment. IEEE Robotics and Automation Letters, March 2024.
[21] Bui CD, Quinn A, Iacopino D, Narbudowicz A. Compact chipless RFID sensor for frozen food monitoring. IEEE Sensors Journal, 2024.

PARTICULARS OF CONTRIBUTORS:
1. Research Scholar, Department of Electrical and Electronics Engineering, Hindustan Institute of Technology and Science, Chennai, Tamil Nadu, India.
2. Professor, Department of Electronics and Communication Engineering, Hindustan Institute of Technology and Science, Chennai, Tamil Nadu, India.

NAME, ADDRESS, E-MAIL ID OF THE CORRESPONDING AUTHOR:
Muralidharan,
No 1, Rajiv Gandhi Salai, Padur, Chennai-603103, Tamil Nadu, India.
E-mail: kmdgct13@gmail.com

PLAGIARISM CHECKING METHODS: [Jain H et al.]
- Plagiarism X-checker: Mar 13, 2025
- Manual Googling: Aug 28, 2025
- iThenticate Software: Aug 30, 2025 (3%)

ETYMOLOGY: Author Origin

EMENDATIONS: 6

AUTHOR DECLARATION:
- Financial or Other Competing Interests: None
- Was Ethics Committee Approval obtained for this study? Yes
- Was informed consent obtained from the subjects involved in the study? Yes
- For any images presented appropriate consent has been obtained from the subjects. No

Date of Submission: **Mar 03, 2025**
Date of Peer Review: **Jun 26, 2025**
Date of Acceptance: **Sep 02, 2025**
Date of Publishing: **Jan 01, 2026**